Nano Nexus & Applications

www.nna.reapress.com

Nano. Nex. App. Vol. 1, No. 3 (2026) 161–177.

Paper Type: Original Article

Flow and Heat Transfer Characteristics of Jet-Assisted Non-Newtonian Nanofluids in Backward-Facing Step Channels

Amir Reza Aghaei*

Department of Mechanical Engineering, Ayandegan University, Tonekabon, Iran; amirreza.aghaei96@gmail.com.

Citation:

Received: 05 January 2026 *Revised: 02 April 2026* *Accepted: 20 May 2026*	Aghaei, A. R. (2026). Flow and heat transfer characteristics of jet-assisted non-Newtonian nanofluids in backward-facing step channels. *Nano Nexus & Applications*, *1*(3), 161-177.

Abstract

This study numerically investigates the thermal-hydraulic performance of a jet-assisted Backward-Facing Step (BFS)channel using a non-Newtonian Al_2O_3/Carboxymethyl Cellulose (CMC) nanofluid under steady-state, laminar, incompressible, and two-dimensional flow conditions. The governing equations of mass, momentum, and energy are solved using the finite volume method, while the rheological behavior of the CMC solution is modeled using the Power-Law model. The numerical model is validated against previously published experimental and numerical data, demonstrating good agreement with benchmark results. The effects of Reynolds number, nanoparticle volume fraction, fluid rheology, jet injection angle, and jet momentum ratio on the flow structure and thermal-hydraulic performance of the channel are systematically investigated. The results reveal that increasing the Reynolds number significantly enhances convective heat transfer by strengthening fluid mixing and reducing the thermal boundary layer thickness. The incorporation of Al_2O_3 nanoparticles improves the overall thermal performance owing to the enhanced effective thermal conductivity of the nanofluid. Furthermore, the shear-thinning behavior of the non-Newtonian CMC solution provides superior heat transfer characteristics compared with Newtonian water. The jet injection parameters are also found to play a critical role in controlling the flow structure and thermal performance of the system. Appropriate jet injection angles and momentum ratios improve fluid mixing and significantly enhance heat transfer while maintaining favorable thermal-hydraulic characteristics. The Performance Evaluation Criterion (PEC) confirms that the combined application of jet injection and non-Newtonian nanofluids offers considerable thermal enhancement with acceptable hydraulic penalties. The findings demonstrate the potential of jet-assisted non-Newtonian Al_2O_3/CMC nanofluids for advanced cooling and thermal management applications involving separated flow configurations.

Keywords: Backward-facing step channel, Non-Newtonian nanofluid, Jet injection, Thermal-hydraulic performance, Heat transfer enhancement, Reynolds number, Jet momentum ratio.

1 | Introduction

Efficient thermal management has become an increasingly important challenge in many engineering applications, including electronic cooling systems, heat exchangers, microfluidic devices, chemical processing

Corresponding Author: amirreza.aghaei96@gmail.com
https://doi.org/10.48314/nna.vi.69

equipment, and energy conversion technologies [1–4]. The continuous demand for compact and high-performance thermal systems has stimulated extensive research on advanced heat transfer enhancement techniques. Conventional cooling approaches are often insufficient to meet the thermal requirements of modern engineering systems, particularly in applications involving high heat fluxes and limited available space. Consequently, the development of passive and active heat transfer enhancement methods has attracted significant attention in recent decades [5].

Among various flow configurations employed in thermal engineering, the Backward-Facing Step (BFS) channel has been widely investigated owing to its unique hydrodynamic characteristics and practical relevance [6–8]. The sudden expansion created by the step geometry induces flow separation and recirculation zones downstream of the step, leading to complex fluid dynamic phenomena such as vortex formation, reattachment, and enhanced fluid mixing [9–11]. These flow characteristics substantially influence both momentum and heat transfer mechanisms within the channel. Because of its simple geometry and well-defined separated flow structure, the BFS configuration has become a benchmark problem for validating numerical methods and investigating thermal enhancement strategies in separated flows [12].

The thermal performance of BFS channels is strongly dependent on the size and behavior of the recirculation region. Flow separation downstream of the step alters the local velocity distribution and significantly affects the development of thermal boundary layers along the heated wall. Appropriate modification of the flow structure can improve fluid mixing and promote convective heat transfer [13]. Therefore, numerous studies have focused on enhancing the thermal-hydraulic performance of BFS channels by introducing various passive and active flow control techniques, including surface modifications, vortex generators, flow obstacles, and fluid injection methods. Among active enhancement techniques, jet injection has emerged as an effective approach for improving heat transfer performance. The injection of a secondary fluid stream into the primary flow can significantly modify the local flow field by increasing momentum exchange and promoting turbulence or fluid mixing, even under laminar flow conditions. Depending on the injection angle, momentum ratio, and jet location, jet injection may alter the recirculation characteristics and thermal boundary layer development within the channel [14–17]. The interaction between the injected jet and the main flow creates favorable conditions for heat transfer enhancement by continuously disrupting the thermal boundary layer and increasing fluid circulation near the heated surface. Consequently, jet-assisted cooling strategies have been successfully employed in numerous thermal management applications [18].

The effectiveness of jet injection is highly dependent on several operating parameters. The jet momentum ratio governs the penetration depth of the injected fluid and determines the strength of its interaction with the main stream. Similarly, the jet injection angle influences the direction of momentum transfer and affects the size and position of the recirculation zones downstream of the step. Optimizing these parameters is therefore essential for achieving maximum thermal performance while minimizing undesirable pressure-drop penalties. Understanding the combined effects of jet injection parameters on separated flows remains an important topic in thermal-fluid sciences [14–21].

In addition to geometric and flow control modifications, improving the thermophysical properties of the working fluid has proven to be an efficient strategy for enhancing heat transfer. Nanofluids, which consist of nanoparticles dispersed within conventional base fluids, have received considerable attention because of their superior thermal properties compared with traditional heat transfer fluids. The addition of nanoparticles can significantly improve the effective thermal conductivity of the fluid and consequently enhance convective heat transfer performance. Aluminum Oxide (Al_2O_3) nanoparticles are among the most extensively investigated nanomaterials owing to their favorable thermal properties, chemical stability, availability, and relatively low cost. Numerous numerical and experimental investigations have demonstrated that Al_2O_3-based nanofluids can provide substantial improvements in heat transfer performance under various flow configurations [22–26].

Although most conventional nanofluid studies have employed Newtonian base fluids such as water, recent advances in thermal engineering have highlighted the advantages of non-Newtonian fluids for specialized heat transfer applications. Non-Newtonian fluids exhibit rheological characteristics that differ significantly from those of Newtonian fluids, allowing them to respond dynamically to variations in shear rate. In particular, shear-thinning fluids exhibit a reduction in apparent viscosity at high shear rates, which may improve fluid circulation and enhance momentum transport in regions of strong flow gradients. These characteristics make non-Newtonian fluids attractive candidates for advanced cooling systems involving complex flow structures and separated flow regions [27].

Carboxymethyl Cellulose (CMC) solutions represent one of the most widely used shear-thinning fluids in engineering and industrial applications. The rheological behavior of CMC solutions can be effectively described using the power-law model and offers desirable thermal-hydraulic characteristics for heat transfer enhancement studies. When combined with thermally conductive nanoparticles, CMC-based nanofluids provide an opportunity to simultaneously exploit enhanced thermal conductivity and favorable rheological behavior. The synergistic interaction between nanoparticle-induced thermal enhancement and shear-thinning flow characteristics can potentially lead to significant improvements in cooling performance [22–29].

The combined application of non-Newtonian nanofluids and jet injection techniques in BFS channels offers considerable potential for thermal performance enhancement. The flow separation naturally present in BFS geometries creates favorable conditions for fluid mixing, while jet injection actively modifies the recirculation zone and thermal boundary layer development. Furthermore, the addition of nanoparticles improves the effective thermal conductivity of the working fluid, and the shear-thinning characteristics of CMC solutions facilitate momentum transport in regions of elevated shear rates. The simultaneous utilization of these mechanisms may provide substantial improvements in heat transfer performance compared with conventional cooling approaches [30–35].

Despite the extensive literature on BFS flows, jet injection techniques, and nanofluid heat transfer enhancement, relatively few studies have investigated the combined influence of jet injection parameters and non-Newtonian nanofluids in separated flow configurations. In particular, the thermal-hydraulic behavior of jet-assisted Al_2O_3/CMC nanofluids in BFS channels has not been comprehensively examined. A systematic investigation of the interactions among Reynolds number, nanoparticle concentration, fluid rheology, jet injection angle, and jet momentum ratio are therefore necessary to provide deeper insights into the mechanisms governing heat transfer enhancement in such systems [32–40].

Accordingly, the present study numerically investigates the thermal and hydrodynamic performance of a BFS channel subjected to jet injection using a non-Newtonian Al_2O_3/CMC nanofluid. The effects of Reynolds number, nanoparticle volume fraction, fluid rheology, jet injection angle, and jet momentum ratio on the flow structure and heat transfer characteristics are systematically examined using the finite volume method. Particular attention is devoted to evaluating the thermal-hydraulic performance of the proposed cooling configuration and identifying the mechanisms responsible for heat transfer enhancement in separated flows.

2|Methodology

2.1|Problem Geometry

The physical model considered in this study consists of a two-dimensional BFS channel equipped with a jet injection system. The computational domain includes a sudden expansion section that induces flow separation and the formation of a recirculation region downstream of the step. A schematic representation of the computational geometry is illustrated in *Fig. 1*. The channel dimensions and the geometric parameters were selected according to the specifications adopted in the present numerical investigation.

The injected jet enters the channel at a prescribed angle relative to the main flow direction and interacts with the separated flow region formed behind the step. This jet-assisted configuration is employed to enhance fluid mixing and improve heat transfer characteristics within the channel. The lower wall downstream of the BFS is subjected to a constant heat flux boundary condition, whereas the upper wall is considered thermally insulated. The combined effects of flow separation, jet injection, and non-Newtonian nanofluid properties are systematically investigated under laminar flow conditions.

2.2 | Thermophysical Properties of the Nanofluid

The working fluid considered in this study is an Al_2O_3/CMC non-Newtonian nanofluid. Aluminum oxide nanoparticles are dispersed within a CMC aqueous solution to improve the thermal performance of the base fluid. The effective thermophysical properties of the nanofluid are evaluated using commonly accepted mixture models.

The effective density of the nanofluid is calculated as (*Eq. (1)*) [31]:

$$\rho_{nf} = (1-\varphi)\rho_f + \varphi\rho_p, \tag{1}$$

where φ denotes the nanoparticle volume fraction, while the subscripts nf, f, and p represent the nanofluid, base fluid, and nanoparticles, respectively.

The effective volumetric heat capacity is determined by (*Eq. (2)*) [30]:

$$(\rho c_P)_{nf} = (1-\varphi)(\rho c_P)_f + \varphi(\rho c_P)_p. \tag{2}$$

The effective thermal conductivity of the nanofluid is evaluated using appropriate correlations available in the literature for Al_2O_3-based nanofluids. The thermophysical properties of water, aluminum oxide nanoparticles, and nanofluids at different nanoparticle volume fractions are adopted from previously published experimental and numerical studies.

2.3 | Rheological Model

The CMC solution exhibits non-Newtonian shear-thinning behavior and therefore cannot be accurately described by Newtonian constitutive relations. The rheological characteristics of the fluid are modeled using the Power-Law model, which has been widely employed for polymeric and non-Newtonian fluids in thermal engineering applications.

The relationship between shear stress and shear rate is expressed as (*Eq. (3)*) [23]:

$$\tau = K\dot{\gamma}^{(n-1)}, \tag{3}$$

where τ is the shear stress, $\dot{\gamma}$ is the shear rate, K denotes the consistency index, and n is the flow behavior index.

The apparent viscosity is calculated using (*Eq. (4)*) [34]:

$$\mu app = K\dot{\gamma}\text{^}(n-1). \tag{4}$$

For values of n less than unity, the fluid exhibits pseudoplastic (shear-thinning) behavior. Under these conditions, the apparent viscosity decreases with increasing shear rate, which can promote fluid circulation and improve momentum transport in regions characterized by strong velocity gradients.

2.4 | Governing Equations

The numerical simulations are performed under steady-state, incompressible, laminar, and two-dimensional flow assumptions. Thermal equilibrium between the nanoparticles and the base fluid is assumed throughout the computational domain.

The conservation equations governing fluid flow and heat transfer consist of the continuity, momentum, and energy equations.

The continuity equation is given by (*Eq. (5)*) [40]:

$$\nabla . V = 0, \quad (5)$$

where V represents the velocity vector.

The momentum equation is expressed as (*Eq. (6)*) [35]:

$$\rho nf(V.\nabla)V = -\nabla P + \nabla(\mu app \nabla V), \quad (6)$$

where P denotes pressure and μapp represents the apparent viscosity obtained from the Power-Law model.

The energy equation can be written as (*Eq. (7)*) [40]:

$$\rho nfCp, nf(V \cdot \nabla T) = \nabla \cdot (knf \nabla T), \quad (7)$$

where T denotes the fluid temperature and knf represents the effective thermal conductivity of the nanofluid.

2.5 | Boundary Conditions

A uniform velocity profile and constant temperature are imposed at the channel inlet. At the outlet boundary, fully developed flow conditions are assumed and all axial gradients are set equal to zero.

The lower wall downstream of the BFS is subjected to a constant heat flux boundary condition, which is expressed as (*Eq. (8)*) [34]:

$$-knf(\frac{\partial T}{\partial y}) = q''. \quad (8)$$

The upper wall is considered adiabatic and satisfies (*Eq. (9)*) [35]:

$$\frac{\partial T}{\partial n} = 0. \quad (9)$$

The no-slip boundary condition is applied to all solid walls, resulting in zero velocity components at the wall surfaces (U=V=0).

The injected jet enters the channel with a prescribed velocity and injection angle. Different jet momentum ratios and injection angles are considered to evaluate their influence on the flow structure and thermal-hydraulic performance of the BFS channel.

2.6 | Numerical Procedure

The governing equations are discretized using the finite volume method (FVM). The computational domain is divided into structured quadrilateral control volumes to accurately capture the flow separation and reattachment phenomena occurring downstream of the BFS.

Pressure-velocity coupling is handled using the SIMPLE algorithm. Convective terms are discretized using second-order upwind schemes, whereas diffusive terms are treated using second-order central differencing. The resulting algebraic equations are solved iteratively until convergence is achieved.

The convergence criteria are defined based on the normalized residuals, with values of 10^{-6} for the continuity and momentum equations and 10^{-8} for the energy equation. All numerical simulations are performed under steady-state conditions [34].

2.7 | Grid Independence Study

To ensure numerical accuracy and eliminate the influence of mesh size on the predicted results, a grid independence analysis is conducted using several structured meshes with progressively increasing numbers of computational cells. The average Nusselt number and reattachment length are selected as the primary monitoring parameters for evaluating mesh sensitivity. The numerical solution is considered grid-independent when the variation between two consecutive mesh refinements becomes less than 1%. The optimum computational mesh is subsequently employed in all simulations to provide an appropriate balance between numerical accuracy and computational efficiency [31].

2.8 | Model Validation

The numerical model is validated against previously published experimental and numerical results available for BFS flows reported in the literature. Comparisons are performed for velocity profiles and Nusselt number distributions under benchmark operating conditions. The predicted results demonstrate good agreement with the available reference data, confirming the reliability and accuracy of the adopted numerical methodology.

The satisfactory agreement between the present simulations and benchmark studies verifies the capability of the developed model to accurately predict flow separation, recirculation behavior, and convective heat transfer characteristics in BFS channels [22].

2.9 | Performance Evaluation Criterion

To evaluate the overall thermal-hydraulic performance of the proposed cooling configuration, the Performance Evaluation Criterion (PEC) is employed. This parameter simultaneously accounts for the enhancement in heat transfer and the associated pressure-drop penalty. The PEC is defined as (*Eq. (10)*) [34]:

$$\mathrm{PEC} = \frac{\mathrm{Nu}/\mathrm{Nu_0}}{\left(\frac{\mathrm{f}}{\mathrm{f_0}}\right)^{1/3}}, \tag{10}$$

where Nu and f denote the average Nusselt number and friction factor corresponding to the enhanced configuration, while $\mathrm{Nu_0}$ and $\mathrm{f_0}$ represent the values associated with the reference case. A PEC value greater than unity indicates that the heat transfer enhancement outweighs the accompanying increase in pressure loss and therefore reflects an overall improvement in thermal-hydraulic performance.

3 | Results & Discussion

3.1 | Validation of the Numerical Model

The accuracy and reliability of the present numerical model were verified by comparing the predicted results with previously published benchmark studies available in the literature. Validation was performed for both heat transfer and flow field characteristics of BFS flows.

Fig. 1.a presents the comparison between the local Nusselt number distribution obtained in the present study and the numerical results reported by Santra et al. [41] for similar operating conditions. As can be observed, an excellent agreement exists between the present predictions and the reference data over the entire computational domain. The close correspondence of the Nusselt number distributions confirms the capability of the adopted numerical approach in accurately predicting convective heat transfer characteristics.

In addition to heat transfer validation, the hydrodynamic behavior of the numerical model was assessed by comparing the velocity profiles with the experimental measurements reported by Armaly et al. [11], as illustrated in *Fig. 1.b*. The predicted velocity distributions at different axial locations downstream of the BFS exhibit very good agreement with the experimental results. The model successfully captures the flow separation, recirculation, and reattachment phenomena that are characteristic of BFS configurations.

The satisfactory agreement between the present numerical results and the available benchmark data demonstrates the accuracy of the finite volume formulation, boundary conditions, and numerical solution procedure employed in this study. Consequently, the developed computational model is considered sufficiently reliable for investigating the effects of Reynolds number, nanoparticle volume fraction, fluid rheology, jet injection angle, and jet momentum ratio on the thermal-hydraulic performance of the BFS channel.

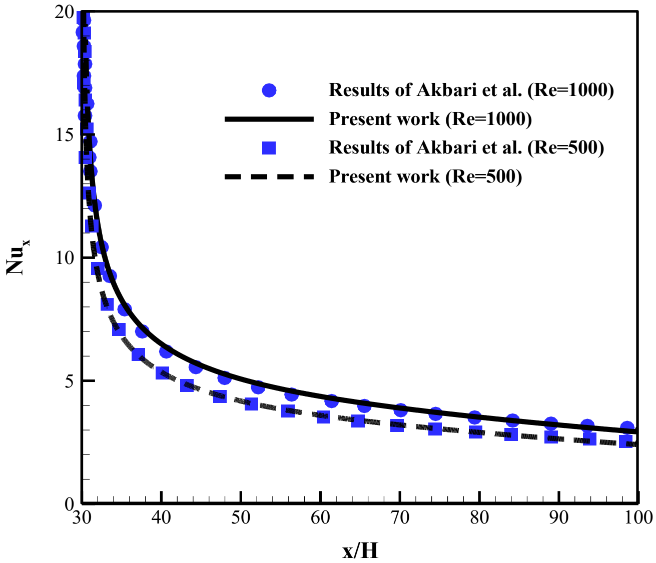

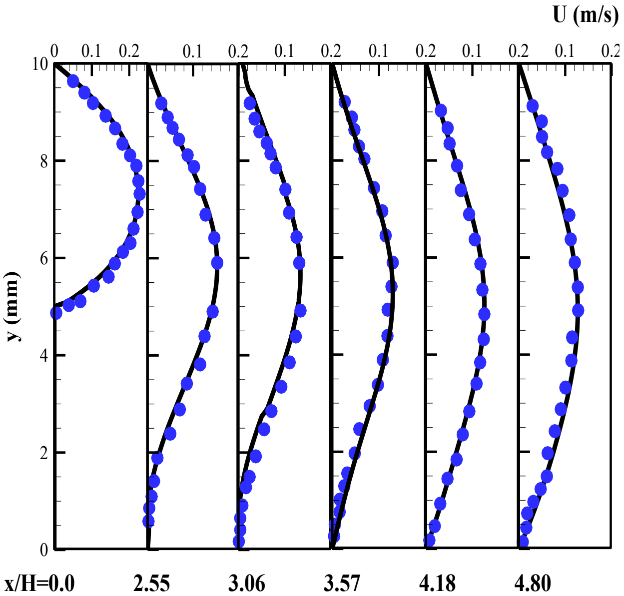

Fig. 1. Validation of the numerical model; a. Nusselt number comparison with Santra et al. [41], and b. velocity profile comparison with the experimental results of Armaly et al. [11].

3.2 | Effect of Reynolds Number

The Reynolds number is one of the most important parameters affecting the flow behavior and heat transfer characteristics in BFS channels. Increasing the Reynolds number intensifies fluid mixing downstream of the step and significantly alters the size and strength of the recirculation region. Consequently, both the hydrodynamic and thermal performances of the channel are strongly influenced by variations in Reynolds number.

Fig. 2.a, b illustrates the streamline patterns obtained at different Reynolds numbers for the jet-assisted non-Newtonian nanofluid flow. As the Reynolds number increases, the flow separation and reattachment phenomena become more pronounced, resulting in stronger recirculation zones downstream of the BFS. The increase in flow inertia enhances momentum transport and promotes fluid mixing within the separated flow region. Moreover, the interaction between the injected jet and the main flow becomes increasingly effective at higher Reynolds numbers, leading to improved circulation near the heated wall.

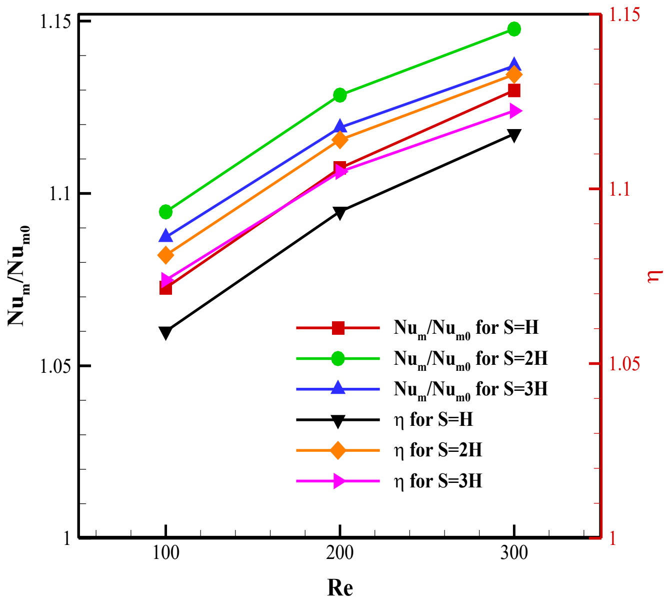

a.

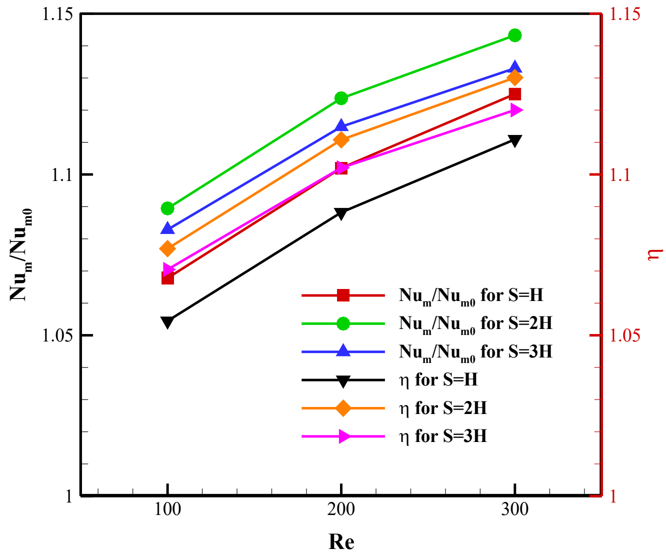

b.

Fig. 2. Streamline patterns of the jet-assisted non-Newtonian nanofluid flow; a. different Reynolds numbers, and b. different Reynolds numbers.

The influence of Reynolds number on the local Nusselt number distribution is presented in *Fig. 3*. It can be observed that increasing the Reynolds number significantly improves the heat transfer performance throughout the channel. Higher Reynolds numbers reduce the thermal boundary layer thickness and increase the wall temperature gradients, resulting in larger local Nusselt numbers. Furthermore, the enhancement in fluid mixing caused by stronger recirculation contributes to more efficient heat removal from the heated surface.

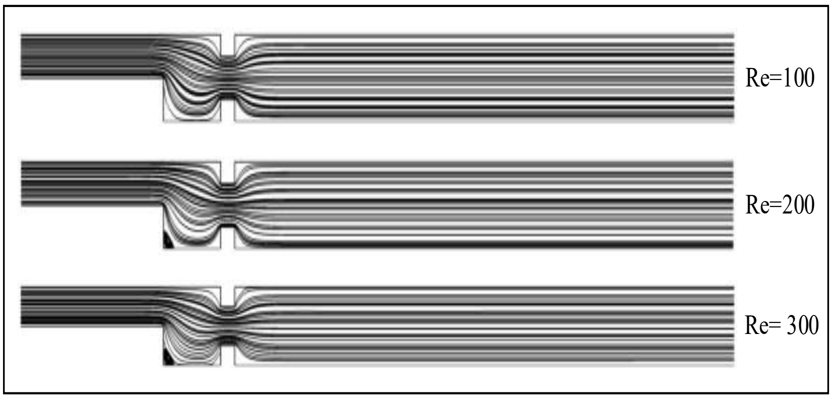

Fig. 3. Local Nusselt number distributions along the heated wall at different Reynolds numbers.

The results indicate that increasing the Reynolds number considerably enhances the thermal performance of the BFS channel. The combined effects of stronger flow recirculation, thinner thermal boundary layers, and improved momentum transport lead to higher convective heat transfer rates. These findings confirm that Reynolds number plays a critical role in determining the thermal-hydraulic behavior of jet-assisted non-Newtonian nanofluid flow in BFS configurations.

3.3|Effect of Nanoparticle Volume Fraction

The nanoparticle volume fraction is an important parameter affecting the thermophysical properties and flow behavior of nanofluids. The addition of nanoparticles modifies the effective thermal conductivity, density, and viscosity of the base fluid, which can influence both the flow structure and heat transfer characteristics in the BFS channel. Therefore, the effect of nanoparticle concentration was investigated by considering different volume fractions of Al_2O_3 nanoparticles under identical operating conditions.

Fig. 4 illustrates the streamline patterns around the BFS for different nanoparticle volume fractions. It can be observed that increasing the nanoparticle concentration slightly influences the flow structure and recirculation characteristics downstream of the step. Although the overall flow pattern remains similar for the investigated cases, variations in nanoparticle concentration modify the effective properties of the nanofluid and consequently affect momentum transport within the channel. The changes in the recirculation region indicate that nanoparticle addition can influence the interaction between the main flow and the separated flow zone.

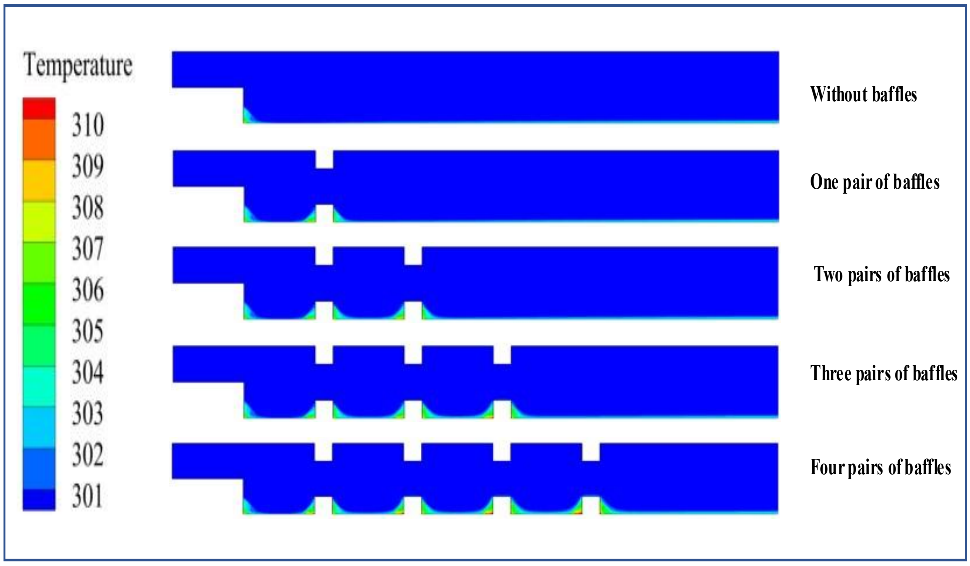

Fig. 4. Streamline patterns around the backward-facing step for different nanoparticle volume fractions (φ = 0.5% and 1.5%) at Re = 300, j = 4, and θ = 0°.

The presence of Al_2O_3 nanoparticles enhances the thermal conductivity of the working fluid, which improves the ability of the nanofluid to transport thermal energy from the heated wall toward the bulk flow region. Although the hydrodynamic structure does not experience significant changes at the investigated nanoparticle concentrations, the improved thermophysical properties contribute to enhanced heat transfer performance. The results confirm that increasing nanoparticle volume fraction is an effective approach for improving the thermal characteristics of non-Newtonian nanofluid flow in BFS channels.

The nanoparticle volume fraction plays an important role in controlling the thermal behavior of the system. The incorporation of Al_2O_3 nanoparticles provides improved heat transfer capability while maintaining the fundamental flow characteristics of the BFS configuration.

3.4 | Effect of Non-Newtonian Behavior

The rheological behavior of the working fluid plays an important role in determining the flow characteristics of BFS channels. Non-Newtonian fluids exhibiting shear-thinning behavior can significantly influence momentum transport and fluid circulation in separated flow regions. Therefore, the effect of fluid rheology was investigated by comparing Newtonian water and a non-Newtonian CMC solution under identical operating conditions.

Fig. 5 presents the streamline patterns around the BFS for Newtonian water and the non-Newtonian CMC solution at Re=300 and j=4. Although both fluids exhibit the characteristic flow separation and recirculation region downstream of the step, noticeable differences in the flow structures can be observed. The non-Newtonian CMC solution exhibits shear-thinning behavior, which reduces its apparent viscosity in regions with high shear rates. Consequently, momentum transport is enhanced near the separation and reattachment zones, resulting in a more favorable flow structure compared with the Newtonian fluid.

The rheological properties of the CMC solution influence the development of the recirculation region and improve fluid circulation within the channel. The reduced viscous resistance in high-shear regions facilitates fluid motion and contributes to more effective interaction between the separated flow and the main stream. Such flow characteristics are beneficial for thermal management applications involving complex channel geometries.

The results demonstrate that the non-Newtonian behavior of the working fluid has a significant influence on the hydrodynamic characteristics of BFS flows. The use of shear-thinning fluids provides improved flow behavior and offers considerable potential for enhancing the performance of advanced cooling systems employing separated flow configurations.

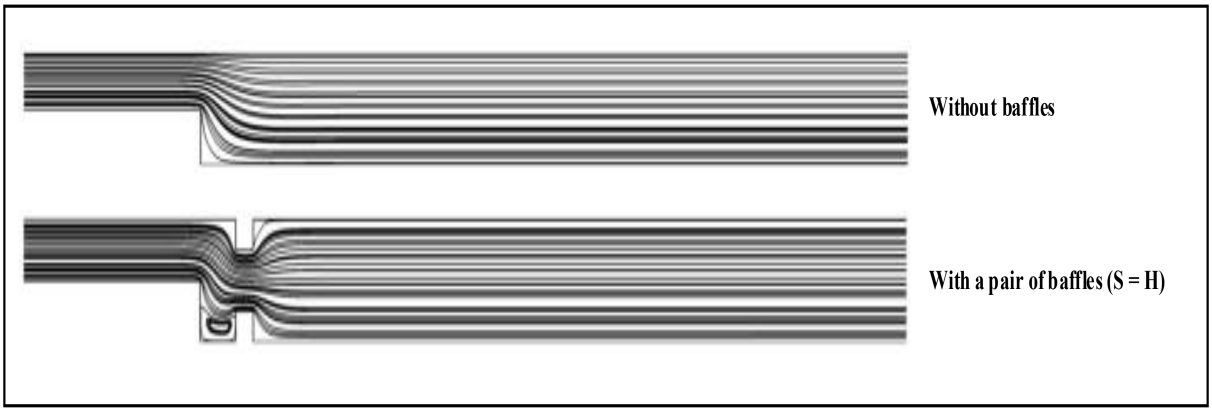

Fig. 5. Streamline patterns for Newtonian water and non-Newtonian CMC solution at Re = 300.

3.5 | Effect of Jet Injection Angle

The jet injection angle is one of the most influential parameters affecting the flow structure and thermal performance of BFS channels. Variations in the injection angle modify the direction of momentum transfer between the injected jet and the main flow, thereby influencing the recirculation characteristics, fluid mixing mechanisms, and heat transfer behavior within the channel. Therefore, an appropriate selection of the jet injection angle is essential for maximizing thermal performance while minimizing hydraulic losses.

Fig. 6 presents the streamline patterns obtained for different jet injection angles. It can be observed that changing the injection angle significantly alters the flow structure downstream of the BFS. Variations in the jet direction modify the interaction between the injected fluid and the main stream, resulting in changes in the size and intensity of the recirculation region. Moreover, the location of flow reattachment is affected by the jet angle, which consequently influences the distribution of velocity and thermal boundary layers along the heated wall. The enhanced fluid mixing produced by favorable jet orientations contributes to improved convective heat transfer performance.

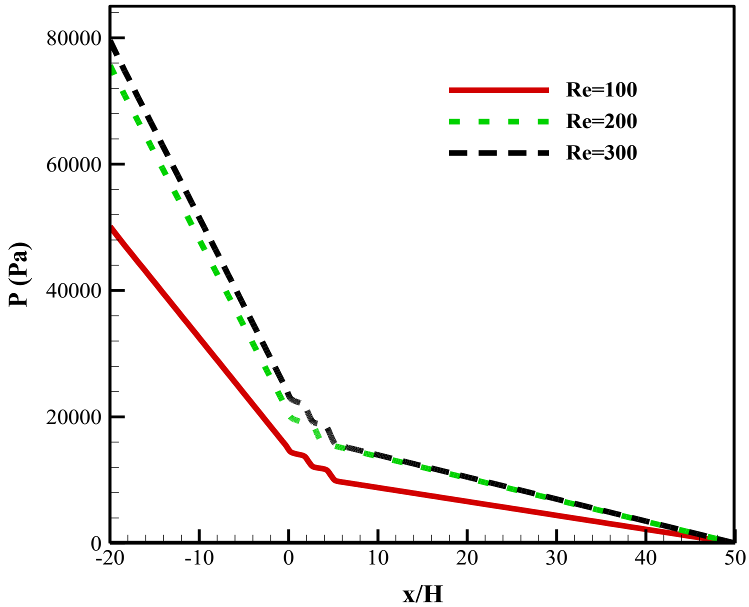

Fig. 6. Streamline patterns for different jet injection angles at Re=300, φ=0.5%, and J=4.

The effect of jet injection angle on heat transfer characteristics is illustrated in *Fig. 7* through the variation of the average Nusselt number at different Reynolds numbers. The results indicate that the jet injection angle considerably affects the convective heat transfer rate within the channel. Appropriate jet orientations promote stronger interaction between the injected flow and the separated flow region, thereby increasing fluid circulation near the heated surface and enhancing thermal transport. Consequently, higher average Nusselt numbers are obtained for the optimum injection angles investigated in this study.

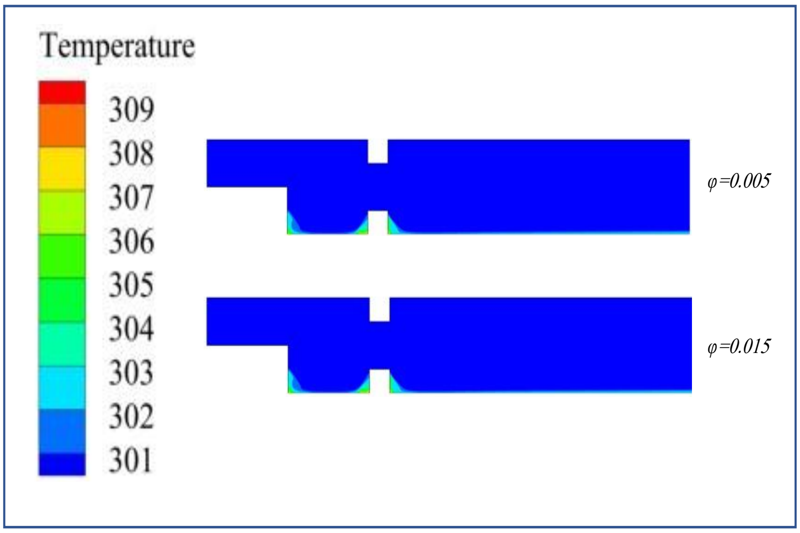

Fig. 7. Variation of average Nusselt number for different jet injection angles at various Reynolds numbers.

The overall thermal-hydraulic performance of the system is evaluated using the PEC, as shown in *Fig. 8*. Although heat transfer enhancement generally improves with favorable jet injection angles, the associated pressure-drop penalty must also be considered. The PEC results demonstrate that specific injection angles provide the most favorable balance between heat transfer enhancement and hydraulic losses. These optimum conditions maximize the overall thermal performance of the BFS channel and highlight the importance of properly selecting the jet injection angle in practical thermal management applications.

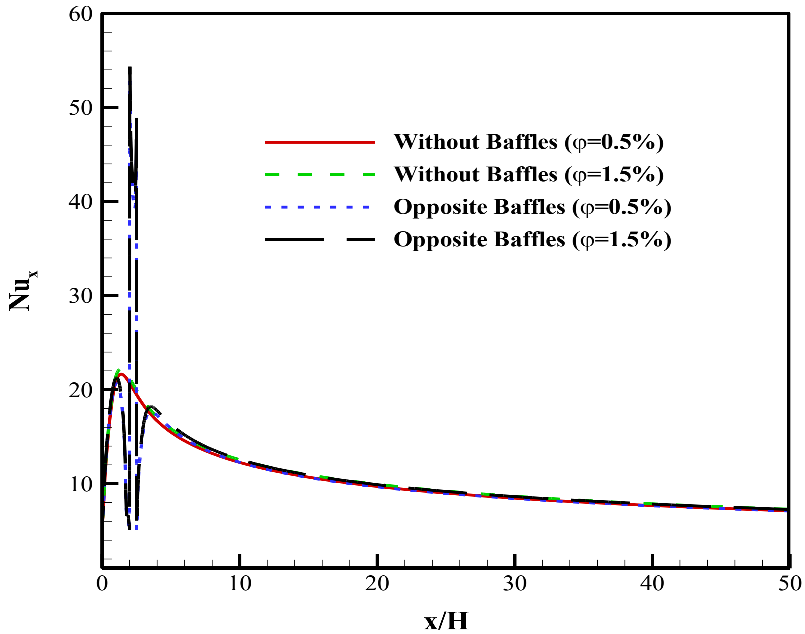

Fig. 8. Variation of the performance evaluation criterion for different jet injection angles at various Reynolds numbers.

The results confirm that the jet injection angle plays a critical role in controlling the separated flow structure and determining the thermal-hydraulic performance of the channel. By appropriately selecting the injection angle, significant improvements in both heat transfer and overall system performance can be achieved.

3.6 | Effect of Jet Momentum Ratio

The jet momentum ratio is one of the most influential parameters governing the interaction between the injected jet and the main channel flow. Variations in the jet momentum ratio significantly affect the jet penetration depth, fluid mixing characteristics, and the thermal behavior of the BFS channel. Therefore, understanding the influence of jet momentum ratio is essential for optimizing the overall thermal-hydraulic performance of jet-assisted cooling systems.

The influence of jet momentum ratio on heat transfer performance is illustrated in *Fig. 9* through the variation of the average Nusselt number at different Reynolds numbers. The results indicate that increasing the jet momentum ratio generally enhances convective heat transfer within the channel. Higher momentum ratios provide the injected jet with greater kinetic energy, allowing it to penetrate further into the main flow and interact more effectively with the recirculation region downstream of the BFS. Consequently, fluid mixing near the heated wall is intensified, leading to thinner thermal boundary layers and larger wall temperature gradients. These mechanisms collectively contribute to higher average Nusselt numbers and improved cooling performance.

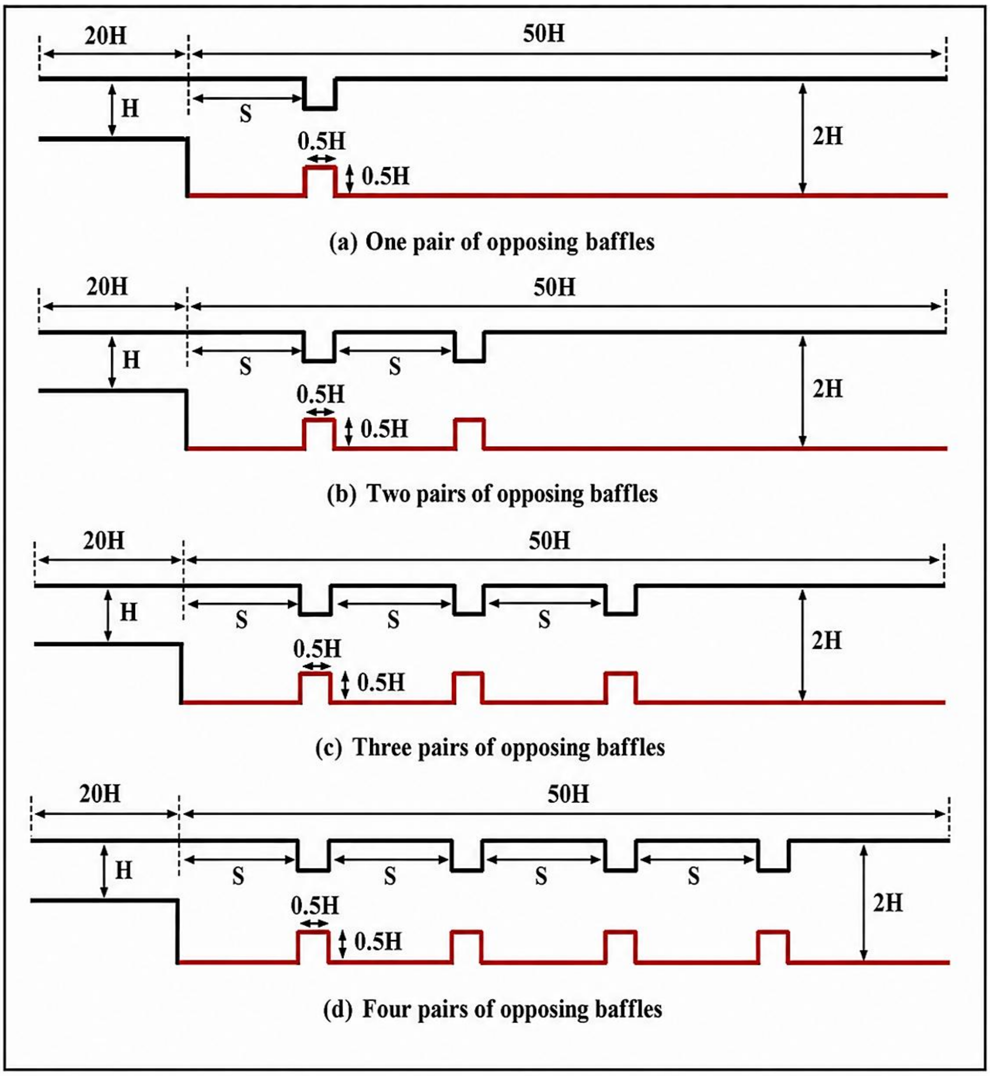

Fig. 9. Variation of average Nusselt number for different jet momentum ratios at various Reynolds numbers.

The overall thermal-hydraulic performance of the system is evaluated using the PEC, as shown in *Fig. 10*. Although increasing the jet momentum ratio improves heat transfer characteristics, excessively large momentum ratios may introduce additional pressure losses due to stronger flow disturbances and increased velocity gradients. The PEC results demonstrate that an optimum range of jet momentum ratios exists in which the heat transfer enhancement outweighs the accompanying hydraulic penalty. Therefore, selecting an appropriate momentum ratio is critical for achieving the most favorable balance between thermal performance and pressure-drop characteristics.

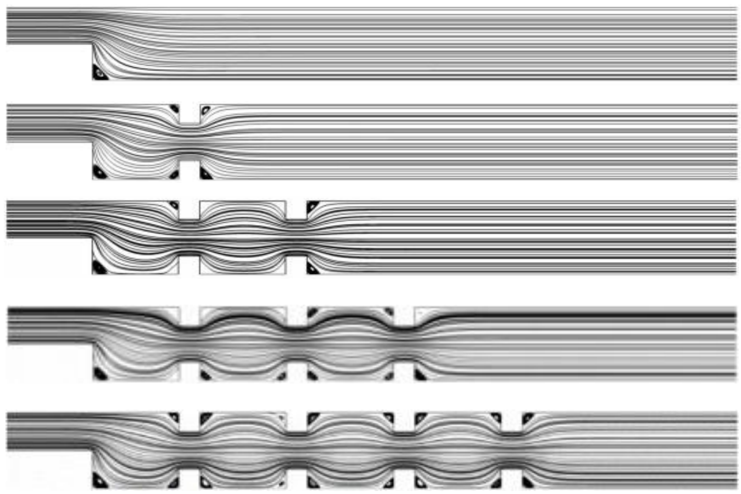

Fig. 10. Variation of the performance evaluation criterion for different jet momentum ratios at various Reynolds numbers.

4 | Conclusion

This study numerically investigated the thermal-hydraulic performance of a jet-assisted BFS channel employing a non-Newtonian Al_2O_3/CMC nanofluid under laminar flow conditions. The effects of Reynolds number, nanoparticle volume fraction, fluid rheology, jet injection angle, and jet momentum ratio on the flow structure and heat transfer characteristics were systematically examined using the finite volume method. The numerical model was successfully validated against previously published experimental and numerical results, demonstrating good agreement and confirming the reliability of the adopted computational methodology. The results revealed that the Reynolds number plays a significant role in enhancing convective heat transfer by intensifying fluid mixing, strengthening the recirculation region, and reducing the thermal boundary layer thickness. Increasing the Reynolds number led to higher Nusselt numbers and consequently improved thermal performance throughout the channel. The influence of nanoparticle volume fraction demonstrated that the incorporation of Al_2O_3 nanoparticles improves the thermal performance of the system. The enhanced effective thermal conductivity of the nanofluid contributed to more efficient heat transfer without significantly altering the main flow characteristics within the investigated operating conditions. The comparison between Newtonian water and the non-Newtonian CMC solution highlighted the beneficial effects of fluid rheology on heat transfer enhancement. The shear-thinning characteristics of the CMC solution promoted improved momentum transport and fluid mixing near the heated wall, resulting in superior convective heat transfer performance compared with the Newtonian case.

Furthermore, the jet injection parameters were found to substantially influence the thermal-hydraulic characteristics of the BFS channel. Variations in the jet injection angle significantly modified the flow structure and recirculation patterns, thereby affecting both heat transfer performance and the overall thermal-hydraulic efficiency. Appropriate jet orientations provided more effective interaction between the injected jet and the main flow, leading to improved cooling performance. Similarly, increasing the jet momentum ratio enhanced jet penetration and intensified fluid mixing within the separated flow region, resulting in higher average Nusselt numbers. However, excessively large momentum ratios may increase hydraulic losses, indicating that an optimum range of momentum ratios exists for achieving the most favorable balance between heat transfer enhancement and pressure-drop penalties.

The combined application of jet injection and non-Newtonian Al_2O_3/CMC nanofluids proved to be an effective strategy for improving the thermal-hydraulic performance of BFS channels. The synergistic effects of enhanced thermal conductivity, shear-thinning rheology, and jet-induced fluid mixing significantly improved convective heat transfer while maintaining acceptable hydraulic characteristics. These findings demonstrate the considerable potential of jet-assisted non-Newtonian nanofluids for advanced cooling and thermal management applications involving separated flow configurations.

Authors' Contributions

All aspects of the research and manuscript preparation were carried out by the author. The author has read and approved the final version of the manuscript.

Data Availability

All data supporting the reported findings in this research paper are provided within the manuscript.

Funding

Not applicable.

Conflict of Interest

The author declares that they do not have any conflict of interest.

Consent for Publication

The author confirms consent for the publication of this work

Ethics Approval and Consent to Participate

This article does not contain any studies with human participants performed by the author.

References

[1] Saldana, J. G. B., Anand, N. K., & Sarin, V. (2005). Forced convection over a three-dimensional horizontal backward facing step. *International Journal for Computational Methods in Engineering Science and Mechanics*, *6*(4), 225–234. https://doi.org/10.1080/155022891009107

[2] Schlichting, H., & Gersten, K. (2016). *Boundary-layer theory*. Springer. https://doi.org/10.1007/978-3-662-52919-5

[3] Xuan, Y., & Li, Q. (2000). Heat transfer enhancement of nanofluids. *International Journal of Heat and Fluid Flow*, *21*(1), 58–64. https://doi.org/10.1016/S0142-727X(99)00067-3

[4] Choi, S. U. S., Zhang, Z. G., Yu, Wl., Lockwood, F. E., & Grulke, E. A. (2001). Anomalous thermal conductivity enhancement in nanotube suspensions. *Applied Physics Letters*, *79*(14), 2252–2254. https://doi.org/10.1063/1.1408272

[5] Paul, G., Philip, J., Raj, B., Das, P. K., & Manna, I. (2011). Synthesis, characterization, and thermal property measurement of nano-Al95Zn05 dispersed nanofluid prepared by a two-step process. *International Journal of Heat and Mass Transfer*, *54*(15–16), 3783–3788. https://doi.org/10.1016/j.ijheatmasstransfer.2011.02.044

[6] Yu, W., France, D. M., Routbort, J. L., & Choi, S. U. S. (2008). Review and comparison of nanofluid thermal conductivity and heat transfer enhancements. *Heat Transfer Engineering*, *29*(5), 432–460. https://doi.org/10.1080/01457630701850851

[7] Kakaç, S., & Pramuanjaroenkij, A. (2009). Review of convective heat transfer enhancement with nanofluids. *International Journal of Heat and Mass Transfer*, *52*(13–14), 3187–3196. https://doi.org/10.1016/j.ijheatmasstransfer.2009.02.006

[8] Das, S. K., Choi, S. U., Yu, W., & Pradeep, T. (2007). *Nanofluids: Science and technology*. John Wiley & Sons. https://www.wiley.com/en-no/shop/nanotechnology-general/nanofluids-science-and-technology-p-9780470180693

[9] Heyhat, M. M., Kowsary, F., Rashidi, A. M., Momenpour, M. H., & Amrollahi, A. (2013). Experimental investigation of laminar convective heat transfer and pressure drop of water-based Al2O3 nanofluids in fully developed flow regime. *Experimental Thermal and Fluid Science*, *44*, 483–489. https://doi.org/10.1016/j.expthermflusci.2012.08.009

[10] Nie, J. H., & Armaly, B. F. (2002). Three-dimensional convective flow adjacent to backward-facing step - effects of step height. *International Journal of Heat and Mass Transfer*, *45*(12), 2431–2438. https://doi.org/10.1016/S0017-9310(01)00345-3

[11] Armaly, B. F., Li, A., & Nie, J. H. (2003). Measurements in three-dimensional laminar separated flow. *International Journal of Heat and Mass Transfer*, *46*(19), 3573–3582. https://doi.org/10.1016/S0017-9310(03)00153-4

[12] Erturk, E. (2008). Numerical solutions of 2-D steady incompressible flow over a backward-facing step, Part I: High Reynolds number solutions. *Computers & Fluids*, *37*(6), 633–655. https://doi.org/10.1016/j.compfluid.2007.09.003

[13] Abdulrazzaq, T., Togun, H., Ariffin, M. K., Kazi, S. N., Badarudin, A., Adam, N. M., & Masuri, S. (2014). Heat transfer and turbulent fluid flow over vertical double forward-facing step. *World Academy of Science, Engineering and Technology*, *86*, 722–726. file:///C:/Users/Administrator/Desktop/9997530.pdf

[14] Moosavi, R., Moltafet, R., & Shekari, Y. (2021). Analysis of viscoelastic non-Newtonian fluid over a vertical forward-facing step using the Maxwell fractional model. *Applied Mathematics and Computation*, *401*, 126119. https://doi.org/10.1016/j.amc.2021.126119

[15] Danane, F., Boudiaf, A., Mahfoud, O., Ouyahia, S. E., Labsi, N., & Benkahla, Y. K. (2020). Effect of backward facing step shape on 3D mixed convection of Bingham fluid. *International Journal of Thermal Sciences*, *147*, 106116. https://doi.org/10.1016/j.ijthermalsci.2019.106116

[16] Poole, R. J., & Escudier, M. P. (2003). Turbulent flow of non-Newtonian liquids over a backward-facing step: Part II. Viscoelastic and shear-thinning liquids. *Journal of Non-Newtonian Fluid Mechanics*, *109*((2-3)), 193–230. https://doi.org/10.1016/S0377-0257(02)00168-4

[17] Ikegami, A., Tsukahara, T., & Kawaguchi, Y. (2015). Influence of viscoelasticity on turbulent flow over a backward-facing step. *Fluids Engineering Division Summer Meeting (vol. 57213, p. v01at25a002)*. American Society of Mechanical Engineers. https://doi.org/10.1115/AJKFluids2015-25251

[18] Boruah, M. P., Pati, S., & Randive, P. R. (2019). Implication of fluid rheology on the hydrothermal and entropy generation characteristics for mixed convective flow in a backward facing step channel with baffle. *International Journal of Heat and Mass Transfer*, *137*, 138–160. https://doi.org/10.1016/j.ijheatmasstransfer.2019.03.094

[19] Ahmed, H. E., & Yusoff, M. Z. (2014). Impact of delta-winglet pair of vortex generators on the thermal and hydraulic performance of a triangular channel using Al2O3–water nanofluid. *Journal of Heat Transfer*, *136*(2), 021901. https://doi.org/10.1115/1.4025434

[20] Pour, M. S., & Nassab, S. G. (2012). Numerical investigation of forced laminar convection flow of nanofluids over a backward facing step under bleeding condition. *Journal of Mechanics*, *28*(2), N7–N12. https://doi.org/10.1017/jmech.2012.45

[21] Togun, H., Safaei, M. R., Sadri, R., Kazi, S. N., Badarudin, A., Hooman, K., & Sadeghinezhad, E. (2014). Numerical simulation of laminar to turbulent nanofluid flow and heat transfer over a backward-facing step. *Applied Mathematics and Computation*, *239*, 153–170. https://doi.org/10.1016/j.amc.2014.04.051

[22] Soltani, S., Etemad, S. G., & Thibault, J. (2010). Pool boiling heat transfer of non-Newtonian nanofluids. *International Communications in Heat and Mass Transfer*, *37*(1), 29–33. https://doi.org/10.1016/j.icheatmasstransfer.2009.08.005

[23] Hojjat, M., Etemad, S. G., & Bagheri, R. (2010). Laminar heat transfer of non-Newtonian nanofluids in a circular tube. *Korean Journal of Chemical Engineering*, *27*(5), 1391–1396. https://doi.org/10.1007/s11814-010-0250-3

[24] Hojjat, M., Etemad, S. G., Bagheri, R., & Thibault, J. (2011). Rheological characteristics of non-Newtonian nanofluids: Experimental investigation. *International Communications in Heat and Mass Transfer*, *38*(2), 144–148. https://doi.org/10.1016/j.icheatmasstransfer.2010.11.019

[25] Chamkha, A. J., & Selimefendigil, F. (2018). Forced convection of pulsating nanofluid flow over a backward facing step with various particle shapes. *Energies*, *11*(11), 3068. https://doi.org/10.3390/en11113068

[26] Mohammed, H. A., Fathinia, F., Vuthaluru, H. B., & Liu, S. (2019). CFD based investigations on the effects of blockage shapes on transient mixed convective nanofluid flow over a backward facing step. *Powder Technology*, *346*, 441–451. https://doi.org/10.1016/j.powtec.2019.02.002

[27] Nath, R., & Krishnan, M. (2019). Numerical study of double diffusive mixed convection in a backward facing step channel filled with Cu-water nanofluid. *International Journal of Mechanical Sciences*, *153–154*, 48–63. https://doi.org/10.1016/j.ijmecsci.2019.01.035

[28] Bobaru, F., & Rachakonda, S. (2004). Optimal shape profiles for cooling fins of high and low conductivity. *International Journal of Heat and Mass Transfer*, *47*(23), 4953–4966. https://doi.org/10.1016/j.ijheatmasstransfer.2004.06.013

[29] Wang, Q. W., Lin, M., & Zeng, M. (2009). Effect of lateral fin profiles on turbulent flow and heat transfer performance of internally finned tubes. *Applied Thermal Engineering*, *29*(14–15), 3006–3013. https://doi.org/10.1016/j.applthermaleng.2009.03.016

[30] Tang, L. H., Zeng, M., & Wang, Q. W. (2009). Experimental and numerical investigation on air-side performance of fin-and-tube heat exchangers with various fin patterns. *Experimental Thermal and Fluid Science*, *33*(5), 818–827. https://doi.org/10.1016/j.expthermflusci.2009.02.008

[31] Yang, M. H., Yeh, R. H., & Hwang, J. J. (2010). Mixed convective cooling of a fin in a channel. *International Journal of Heat and Mass Transfer*, *53*(4), 760–771. https://doi.org/10.1016/j.ijheatmasstransfer.2009.10.012

[32] Mushatet, K. S. (2011). Simulation of turbulent flow and heat transfer over a backward facing step with ribs turbulators. *Thermal Science*, *15*(1), 245–255. https://thermalscience.rs/pdfs/papers/TSCI090926044M.pdf

[33] Mohammed, H. A., Alawi, O. A., & Wahid, M. A. (2015). Mixed convective nanofluid flow in a channel having backward-facing step with a baffle. *Powder Technology*, *275*, 329–343. https://doi.org/10.1016/j.powtec.2014.09.046

[34] Alawi, O. A., Mohammed, H. A., & Sidik, N. C. (2016). Mixed convective nanofluids flow in a channel having forward-facing step with baffle. *Journal of Advanced Research in Applied Mechanics*, *24*(1), 1–21. https://www.akademiabaru.com/submit/index.php/aram/article/view/1759

[35] Ma, Y., Mohebbi, R., Rashidi, M. M., Yang, Z., & Fang, Y. (2020). Baffle and geometry effects on nanofluid forced convection over forward-and backward-facing steps channel by means of lattice Boltzmann method. *Physica A: Statistical Mechanics and Its Applications*, *554*, 124696. https://doi.org/10.1016/j.physa.2020.124696

[36] Heshmati, A., Mohammed, H. A., & Darus, A. N. (2014). Mixed convection heat transfer of nanofluids over backward facing step having a slotted baffle. *Applied Mathematics and Computation*, *240*, 368–386. https://doi.org/10.1016/j.amc.2014.04.058

[37] Amiri, A., Arzani, H. K., Kazi, S. N., Chew, B. T., & Badarudin, A. (2016). Backward-facing step heat transfer of the turbulent regime for functionalized graphene nanoplatelets based water–ethylene glycol nanofluids. *International Journal of Heat and Mass Transfer*, *97*, 538–546. https://doi.org/10.1016/j.ijheatmasstransfer.2016.02.042

[38] Patankar, S. (2018). *Numerical heat transfer and fluid flow*. CRC press. https://doi.org/10.1201/9781482234213

[39] Abu-Nada, E. (2008). Application of nanofluids for heat transfer enhancement of separated flows encountered in a backward facing step. *International Journal of Heat and Fluid Flow*, *29*(1), 242–249. https://doi.org/10.1016/j.ijheatfluidflow.2007.07.001

[40] Mosavi, A., Hekmatifar, M., Alizadeh, A. ad, Toghraie, D., Sabetvand, R., & Karimipour, A. (2020). RETRACTED: The molecular dynamics simulation of thermal manner of Ar/Cu nanofluid flow: The effects of spherical barriers size. *Journal of Molecular Liquids*, *319*, 114183. https://doi.org/10.1016/j.molliq.2020.114183

[41] Santra, A. K., Sen, S., & Chakraborty, N. (2008). Study of heat transfer augmentation in a differentially heated square cavity using copper--water nanofluid. *International Journal of Thermal Sciences*, *47*(9), 1113–1122. https://doi.org/10.1016/j.ijthermalsci.2007.10.005